

DFREC: DeepFake Identity Recovery Based on Identity-aware Masked Autoencoder

Peipeng Yu, Hui Gao, Zhitao Huang, Zhihua Xia, *Member, IEEE*, Chip-Hong Chang, *Fellow, IEEE*

Abstract—Recent advances in deepfake forensics have primarily focused on improving the classification accuracy and generalization performance. Despite enormous progress in detection accuracy across a wide variety of forgery algorithms, existing algorithms lack intuitive interpretability and identity traceability to help with forensic investigation. In this paper, we introduce a novel DeepFake Identity Recovery scheme (DFREC) to fill this gap. DFREC aims to recover the pair of source and target faces from a deepfake image to facilitate deepfake identity tracing and reduce the risk of deepfake attack. It comprises three key components: an Identity Segmentation Module (ISM), a Source Identity Reconstruction Module (SIRM), and a Target Identity Reconstruction Module (TIRM). The ISM segments the input face into distinct source and target face information, and the SIRM reconstructs the source face and extracts latent target identity features with the segmented source information. The background context and latent target identity features are synergetically fused by a Masked Autoencoder in the TIRM to reconstruct the target face. We evaluate DFREC on six different high-fidelity face-swapping attacks on FaceForensics++, CelebaMegaFS and FFHQ-E4S datasets, which demonstrate its superior recovery performance over state-of-the-art deepfake recovery algorithms. In addition, DFREC is the only scheme that can recover both pristine source and target faces directly from the forgery image with high fidelity.

Index Terms—Article submission, IEEE, IEEEtran, journal, LATEX, paper, template, typesetting.

I. INTRODUCTION

THE emergence of deepfake technology, particularly its face-swapping capabilities, has ushered in an unprecedented era of digital media manipulation. It enables the seamless substitution of one individual’s face with another’s. Since its inception, deepfake has rapidly evolved into tools for disseminating misinformation, identity theft, and fraud. The growing ethical and legal concerns on the widespread dissemination of deepfake content have underscored the urgency of developing robust deepfake forensic tools. This is crucial not only for safeguarding individuals’ rights but also upholding the information integrity in the digital age.

Most of the existing deepfake forensic methods focus on improving the generalization detection performance across various kinds of forgery images [1]–[6]. Despite their commendable performance, detection-based algorithms are limited to providing classification or localization results. They lack the capability to provide a corresponding chain of evidence to match the detection result. In other words, they cannot

Peipeng Yu, Hui Gao, Zhitao Huang, and Zhihua Xia are with College of Cyber Security, Jinan University, Guangzhou, 510632, China. Chip-Hong Chang is with the School of Electrical and Electronic Engineering, Nanyang Technological University, Singapore 639798.

Corresponding authors: Zhihua Xia and Chip-Hong Chang. (e-mail: xia_zhihua@163.com, echchang@ntu.edu.sg)

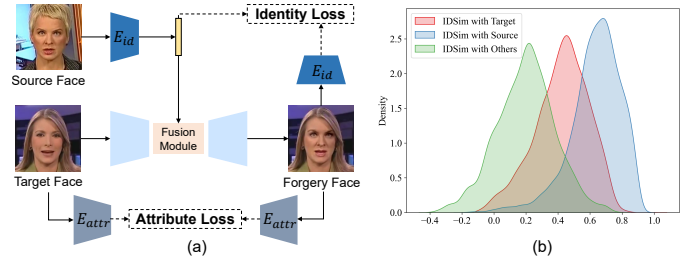


Fig. 1. (a) The training process of deepfake face swapping models. The identity loss is used to increase the similarity between the forgery and source face identities, and the attribute loss is used to ensure the similarity between the forgery and target face attributes. (b) The probability density functions of the identity similarity (IDSim) between the forgery and source, forgery and target, and forgery and other unrelated faces.

trace which are the two faces that have been swapped. The inability to trace the origin of deepfake content can delay timely action and reduce the effectiveness of incident response plan to mitigate potential damage. More importantly, as the onus of proof is borne by the victims with source identities, an accurate recovery of the source and target identities could provide an irrefutable evidence of manipulation. The recovered faces can help to protect the victim from potential hazards and in collecting and identifying evidences for pursuing legal action against the defendant responsible for creating and disseminating deepfake content with malicious intent.

Motivated by this forensic investigation gap, we propose to approach the deepfake forensic task from the perspective of pristine face recovery. While deepfake algorithms have evolved through various iterations, their core operation involves transferring the source identity onto the target face while retaining the attributes of the target face (such as expression, pose, lighting, etc.). This synthesis process inadvertently blends the identities of both faces, resulting in a composite image that incorporates features from both identities [7]. As illustrated in Figure 1, the identity similarity between the forgery face and the target face is closely resembling the similarity between the forgery face and the source face. This observation suggests that the forgery face encompasses a portion of the target face information. Building on this insight, we propose DFREC, a DeepFake Identity Recovery scheme based on Identity-aware Masked autoencoder, which is designed to recover both the source and target faces. The main contributions of this paper are outlined as follows:

- We propose a digital forensic aid DFREC to restore the identities of both target and source faces. DFREC accomplishes this task through (i) designing an Identity Segmentation Module (ISM) to segment information

related to the source and target faces respectively, (ii) constructing a Source Identity Recovery Module (SIRM) to recover the source face using the segmented source information, and (iii) designing a Target Identity Recovery Module (TIRM) to recover the target face using the background information and identity features extracted by the SIRM. Through identity segmentation and recovery, DFREC is able to restore the pristine source and target faces with high fidelity for intuitive interpretation.

- We propose an Identity-aware Masked Autoencoder (MAE) to integrate latent target identity features into the face recovery process. Specifically, the MAE utilizes segmentation maps generated by the ISM to mask the input image and uses the Vision Transformer (ViT) for feature extraction. The target identity features are incorporated into the visible patch embedding to guide the MAE to restore pristine quality image with the desired target face identity.
- We evaluate DFREC on the FaceForensics++, CelebMegaFS, and FFHQ-E4S datasets, across six types of deepfake face swapping approaches. Compared to existing face inpainting methods and deepfake recovery methods, our approach achieves superior face recovery performance. By successfully recover both the pristine source and target faces with the correct identities, DEREK provides a non-repudiable intrinsic evidence of provenance that is gleaned directly from the forgery image.

II. RELATED WORKS

A. Deepfake Face Swapping

Face swapping is a representative algorithm in deepfake technology. It can be categorized into source-oriented and target-oriented methods. Source-oriented methods primarily involve warping the source face to align with the target's pose and expression before it is seamlessly merged into the target frame [8]–[10]. Target-oriented methods, on the other hand, leverage generative models to encode target features and synthesize the swapped face [11]–[16]. It is worth noting that these face swapping algorithms produce high-fidelity forgery face by preserving target's face attributes (such as expression and pose). Due to the inherent difficulty in decoupling identity features from attribute features, the extracted attribute features often exhibit a certain degree of correlation with identity [7]. This inherent correlation often leads to a fusion of source and target identities. Inspired by this insight, our proposed DFREC scheme extracts latent identity features from forgery images to recover the source and target faces, thereby enabling the tracing of both source and target identities.

B. Deepfake Forgery Detection

Deepfake forgery detection predominantly utilizes CNN-based methodologies, and focus more on the generalization performance in recent years. Generalization through diverse strategies, including data augmentation [1], [17], [18], feature consistency analysis [19], [20], and frequency domain anomalies [21], [22] have been explored in recent years to detect fine-grained photorealistic face forgery. Despite their

high detection accuracy, these forensic tools cannot trace the origin of deepfake content, which prevents the victims from pursuing legal action and initiating timely incident response to minimize damage.

C. Deepfake Recovery

Different from detection-based methods, deepfake recovery methods aim to reconstruct the original target face. To improve the identity-relevant deepfake detection and interpretability, RECCE [23] proposed a reconstruction learning approach to discern compact real data representations. Delocate [24] utilized a Masked Autoencoder to reconstruct original facial components to assist in deepfake detection. Additionally, DFI [25], [26] proposed to trace the original target face for interpretable deepfake detection. However, RECCE and Delocate are limited to generating distorted facial images and cannot effectively recover the target identity from the forgery face. DFI cannot avoid the disturbance of source identities on the recovered target faces. To tackle these limitations, we first segment the two types of information within forgery faces to mitigate their interference, and then integrate the background information with the implicit target identity features to recover the deepfake identity.

III. THE PROPOSED METHOD

Deepfake face swapping images contain both the identity of the source face and some attributes of the target face (expression, pose, lighting, etc.). Given the existence of correlation between attributes and identity, we believe that the source and target identities of a face-swapped image can be segregated to allow for the reconstruction of both the source and target faces.

We name our proposed deepfake identity recovery scheme DFREC. As illustrated in Figure 2, DFREC consists of three components: an Identity Segmentation Module (ISM), a Source Identity Reconstruction Module (SIRM), and a Target Identity Reconstruction Module (TIRM). The ISM classifies each pixel of an input image according to its probability of affiliation with the source face. By taking the dot product between the input image and the output probability map, the segmented source face information is produced. The SIRM reconstructs the source face and extracts the target identity features from the decomposed source face information simultaneously. The TIRM masks the image using the segmentation map and recovers the target face by combining the background information with the target identity features. A quadruple loss that combines Identity Loss, Perceptual Loss, Attribute Loss and Patch Recovery Loss is used to guide the face recovery to achieve state-of-the-art (SOTA) recovery quality of the source and target faces.

A. Identity Segmentation Module (ISM)

The ISM is designed to segment source and target face information embedded in a face-swapping image. Specifically, we employ the DeepLabv3 architecture based on atrous convolution, which consists of a feature extractor, a segmentation

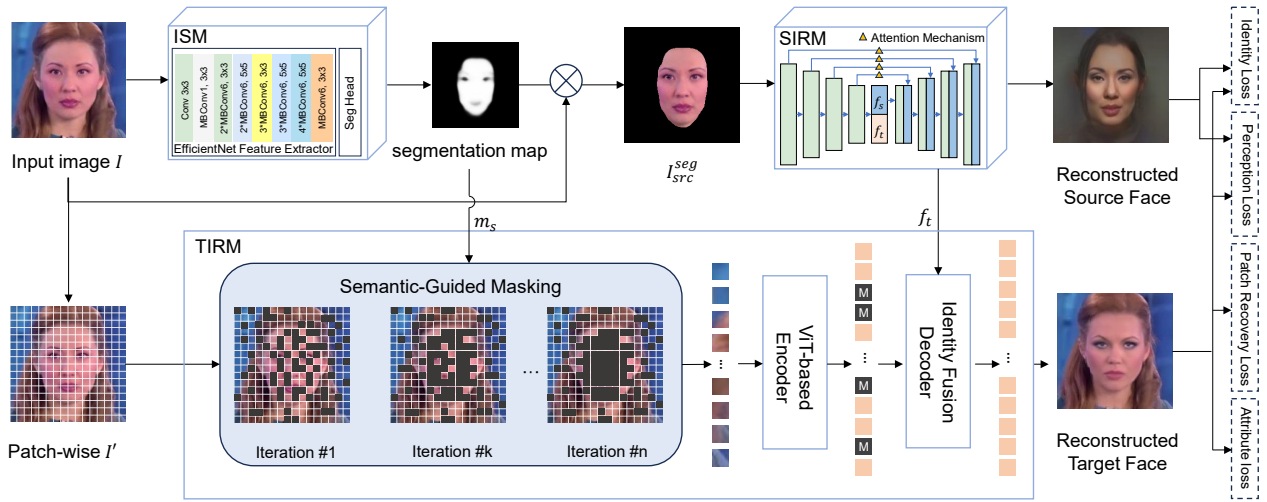


Fig. 2. An overview of DFREC. The Identity Segmentation Module (ISM) segments an input image to extract the source and target information. The Source Identity Recovery Module (SIRM) and Target Identity Recovery Module (TIRM) recover the source and target identities, respectively.

head and a classification head. The classification head determines if an input facial image is a pristine or a forgery face while the segmentation head produces a probabilistic map for the extraction of source face information. We use pretrained EfficientNet-B0 as in [27] to extract both low-level and high-level features. The high-level features are then directed into the classification head for forgery classification. Meantime, the high-level features are supplied to the segmentation head for up-sampling and combined with the low-level features to generate the segmentation map. As illustrated in Figure 2, it takes the image I as input and generates a segmentation map m_s . This map is used to produce a segmented image I_{src}^{seg} for source face recovery as well as guide the MAE to iteratively mask source-related patches for the target face recovery. It is worth noting that we refrain from utilizing any loss function to constrain the segmentation process, as it will autonomously compute the necessary information driven by subsequent tasks.

B. Source Identity Recovery Module (SIRM)

The SIRM is designed to recover the source face and extract the latent target identity features using the segmented I_{src}^{seg} . Specifically, we construct a UNet-like model for source face recovery. As depicted in Figure 2, the SIRM is made up of an encoder and a decoder. The encoder is responsible for identity feature extraction. The extracted identity features are then utilized by the decoder for the source face recovery. Due to the fusion of two identities, features extracted by the encoder may inevitably contain some target face features. This may detrimentally mislead the source face recovery. To address this problem, the features extracted by the encoder are divided into two parts: source identity feature f_s and target identity feature f_t . The separated f_s is independently exploited by the decoder for the recovery of the source face, and the separated f_t is utilized for subsequent target face recovery. An attention mechanism is then introduced into the skip connection to preserve features pertinent to the source face.

Finally, the source face is reconstructed from the segmented source information.

C. Target Identity Recovery Module (TIRM)

The TIRM is devised to recover the target face image. Given that deepfake face swapping algorithms aim to eliminate as much of the target identity from the swapped image as possible, restoring the target face poses more challenges than restoring the source face. To tackle this issue, we introduce an Identity-aware Masked Autoencoder (MAE) to combine the background information and the predicted target identity features to recover the target face. As illustrated in Figure 2, the TIRM comprises two stages: Semantic-Guided Masking and Identity Recovery.

Semantic-Guided Masking: This stage masks a fixed proportion of patches under the guidance of the predicted segmentation map m_s . Traditional MAE-based methods typically mask image patches randomly, and then use visible patches to recover the masked patches. However, most of the forged regions are concentrated around the facial area. Random masking has high propensity to preserve some strong forged facial components that can mislead the target face recovery process. We mitigate this problem by using the predicted m_s to select image patches to be masked. As demonstrated in Algorithm 1, we first segment m_s into n patches, each of size ρ . Each patch is weighted by its average value. For patches with weights less than 0.5, their weights are replaced by random numbers between 0 and 0.1. Then, the patch weights are sorted in descending order. The top m highest weight patches are selected, where the number of patches to be masked m is determined by the mask ratio λ . This strategy gradually shifts the patch masking from random to source-related areas as the accuracy of the predicted segmentation map improves. Eventually, all patches related to the source face will be masked and inpainted by using other visible patches to restore the target face.

Algorithm 1 Semantic-Guided Masking Algorithm

Require: Segmentation map m_s , patch size ρ , mask ratio λ
Ensure: Indices of the masked and kept patches.

- 1: Divide m_s into n patches of size ρ : $P \leftarrow \text{Divide}(m_s, \rho)$;
 - 2: Calculate mean value of m_s : $\mu \leftarrow \text{mean}(m_s)$;
 - 3: Calculate mean value of each patch: $\omega_i \leftarrow \text{mean}(P_i)$;
 - 4: Generate random vector: $\nu \leftarrow \text{RandVector}(n)$;
 - 5: **if** $\mu \geq 0.9$ **then**
 - 6: $\omega \leftarrow \nu$
 - 7: **end if**
 - 8: **for** $i = 1$ to n **do**
 - 9: **if** $\omega_i < 0.5$ **then**
 - 10: $\omega_i \leftarrow \nu_i$
 - 11: **end if**
 - 12: **end for**
 - 13: Get sorted indices of patch weights: $\iota \leftarrow \text{argsort}(\omega)$
 - 14: Calculate number of masked patches: $m \leftarrow n \times \lambda$
 - 15: Get indices of masked patches: $\iota_m \leftarrow \text{Top}_m(\iota)$
 - 16: Get indices of patches to keep: $\iota_k \leftarrow \text{Last}_{n-m}(\iota)$
-

Identity Recovery: The aim of this step is to restore the masked patches to the corresponding patches in the target face. We utilize the background contextual information and the latent target identity information to achieve this objective. Background context information refers to the unmasked patches within the input image, where structural and color correlations among various image components exist. These correlations between pixels or regions can assist in predicting partial information about the masked areas from the unmasked patches. The target identity information is the latent features f_t extracted by the SIRM to guide the reconstruction of the target face. To synergize the background context information with the latent target identity information, we construct an Identity Fusion Decoder in the MAE. The target identity features and visible patch embeddings are concatenated to predict the masked patches. Its principal operations are delineated as follows.

The input image I is first tokenized into a sequence of N tokens $\{x_i^s\}_{i=1}^N$, where N denotes the total number of image patches. For the masked version of I , the visible patch tokens are represented as x^{sv} . Similarly, the target face image I_{tgt} is also tokenized into a sequence of N image patch tokens $\{x_i^t\}_{i=1}^N$. Following the same MAE settings as [28], we utilize a ViT as the encoder G_{enc}^t , and incorporate multiple cascaded transformer blocks as the Identity Fusion Decoder G_{dec}^t . The visible tokens x^{sv} are encoded into token embeddings using linear transformation l , followed by the addition of positional encoding p^{sv} . We feed the fused embeddings into the ViT to obtain the embedding features, which are then concatenated with f_t to generate the token embeddings with identity features. The fused features are fed into the Identity Fusion Decoder to predict the pixels of the masked patches.

$$x^{recm} = G_{dec}^t(G_{enc}^t(l(x^{sv}) + p^{sv}) \parallel f_t) \quad (1)$$

D. Loss Functions

Identity Loss. This loss is computed by subjecting the original and recovered faces to the FaceNet model [29] pretrained on the VGGFace2 dataset [30] to extract their multi-layer identity features. The identity losses for the source and target recovery are calculated as follows:

$$\mathcal{L}_{srcid} = \sum_{i=1}^4 \|E_{id}^i(I_{src}) - E_{id}^i(I_{src}^{rec})\|_2, \quad (2)$$

$$\mathcal{L}_{tgtid} = \sum_{i=1}^4 \|E_{id}^i(I_{tgt}) - E_{id}^i(I_{tgt}^{rec})\|_2, \quad (3)$$

where $E_{id}^i(\cdot)$ denotes the i -th layer features of FaceNet. The four layers of features are extracted from *Mixed_6a*, *repeat_3_block8*, and *last_bn*. I_{src} and I_{tgt} represent the original source and target faces, respectively while I_{src}^{rec} and I_{tgt}^{rec} represent the reconstructed source and target faces, respectively. The overall identity loss is:

$$\mathcal{L}_{id} = \mathcal{L}_{srcid} + \alpha \mathcal{L}_{tgtid}, \quad (4)$$

Perceptual Loss: The perceptual loss between the original and recovered faces is computed using the VGG19 model pretrained on the ImageNet [31] dataset as follows:

$$\mathcal{L}_{srcperc} = \sum_{i=1}^5 \|\psi_i(I_{src}) - \psi_i(I_{src}^{rec})\|_2, \quad (5)$$

$$\mathcal{L}_{tgtperc} = \sum_{i=1}^5 \|\psi_i(I_{tgt}) - \psi_i(I_{tgt}^{rec})\|_2, \quad (6)$$

where $\psi_i(\cdot)$ denotes the i -th layer features of VGG19, and these five layers are *relu1_2*, *relu2_2*, *relu3_4*, *relu4_4*, and *relu5_4*. The overall perceptual loss is:

$$\mathcal{L}_{perc} = \mathcal{L}_{srcperc} + \beta \mathcal{L}_{tgtperc}, \quad (7)$$

Attribute Loss. We utilize the attribute extraction model [32] pretrained on the CelebA dataset [33] to extract the facial attributes of both the recovered and pristine target faces, and use L1 smooth distance to measure their mismatch.

$$\mathcal{L}_{attr} = \begin{cases} 0.5(\mathcal{A}_{tgt} - \mathcal{A}_{rec})^2, & \text{if } |\mathcal{A}_{tgt} - \mathcal{A}_{rec}| < 1 \\ |\mathcal{A}_{tgt} - \mathcal{A}_{rec}| - 0.5, & \text{otherwise} \end{cases}, \quad (8)$$

where \mathcal{A}_{tgt} and \mathcal{A}_{rec} denote the extracted attributes of the pristine target face and the recovered target face, respectively. **Patch Recovery Loss.** Unlike the traditional objective of image reconstruction with the MAE, the TIRM aims to recover the target face. This is achieved by calculating the L2 distance between the recovered patches and the corresponding patches of the target face image.

$$\mathcal{L}_{patch} = \sum_{i=1}^{N_p} \|x_i^{tm} - x_i^{recm}\|_2, \quad (9)$$

where x_i^{tm} and x_i^{recm} represent the i -th masked patches of the pristine target face and the recovered target face, respectively. N_p denotes the number of masked patches.

Overall Loss. The overall loss of DFREC can be summarized as follows.

$$\mathcal{L} = \mathcal{L}_{id} + \lambda_1 \mathcal{L}_{perc} + \lambda_2 \mathcal{L}_{attr} + \lambda_3 \mathcal{L}_{patch}, \quad (10)$$

where λ_1 , λ_2 , and λ_3 are the weight parameters for balancing multiple loss functions.

TABLE I
PERFORMANCE COMPARISON OF THE PROPOSED DFREC WITH SOTA INPAINTING AND DEEFAKE RECOVERY METHODS AGAINST DIFFERENT FACE-SWAPPING FORGERIES ON FACEFORENSICS++, CELEBAMEGAFS AND FFHQ-E4S DATASETS.

Method	FaceForensic++						CelebaMegaFS						FFHQ-E4S	
	DeepFake		FaceShifter		LCR		FTM		IDInjection		LCR		E4S	
	FID ↓	IDSIm ↑	FID ↓	IDSIm ↑	FID ↓	IDSIm ↑	FID ↓	IDSIm ↑	FID ↓	IDSIm ↑	FID ↓	IDSIm ↑	FID ↓	IDSIm ↑
None	11.35	0.4238	8.43	0.4252	22.09	0.3516	11.60	0.2792	10.83	0.3150	12.58	0.2318	8.04	0.2812
MAT	21.01	0.4372	19.23	0.3874	26.98	0.4026	42.06	0.3928	34.64	0.4203	35.98	0.3506	9.82	0.2797
Repaint	21.44	0.3832	19.49	0.3366	27.52	0.3639	41.18	0.3874	33.97	0.3893	35.11	0.3423	38.97	0.3946
RECCE	87.28	0.3755	65.72	0.4400	89.33	0.4086	90.36	0.2547	115.35	0.2957	110.69	0.2313	81.82	0.2668
Delocate	18.16	0.4749	37.22	0.4551	135.93	0.3858	40.75	0.4201	39.90	0.4650	41.76	0.3466	36.88	0.3064
DFI	42.17	0.4706	30.39	0.5207	37.03	0.4860	22.19	0.4137	22.20	0.4346	29.30	0.3442	29.86	0.3805
Ours	17.22	0.5367	18.48	0.5047	27.92	0.5135	15.35	0.7192	13.78	0.7582	14.75	0.6967	8.34	0.5870

IV. EXPERIMENTS

In this section, we first compare the proposed DFREC scheme with the existing SOTA approaches, and then perform an ablation study to demonstrate the effects of each module.

A. Experimental Settings

1) *Datasets*: We utilize three deepfake datasets to train and validate the performance of our scheme. For FaceForensics++ [34], we select two existing forgeries, namely DeepFake (DF) and FaceShifter (FShi). Additionally, we generate another forgery set using the LCR algorithm [35]. The three types of forgery images are then splitted into their corresponding training, validation, and testing images according to the splitting strategy in [34]. CelebaMegaFS [35] incorporates three deepfake methods: IDInjection (IDI), FTM, and LCR, resulting in 30,038 FTM images, 30,441 IDInjection images, and 30,010 LCR images. FFHQ-E4S [16] is constructed based on the FFHQ dataset [36]. We randomly select 10,000 images from FFHQ and use E4S [16] to generate 10 swapped images per original image. For CelebaMegaFS and FFHQ-E4S, each dataset is divided into the training, validation, and test sets according to an 8:1:1 ratio. In the FaceForensics++ and FFHQ-E4S datasets, the identities in the training and testing sets are non-overlapping. In CelebaMegaFS, about 70% of the test identities overlap with the training set.

2) *Compared approaches*: We compare DFREC with five SOTA methods. MAT [37] is a mask-aware transformer for large hole image inpainting, which combines transformers and convolutions to reconstruct high resolution images. RePaint [38] is a face inpainting method which uses a pretrained unconditional Denoising Diffusion Probabilistic Model (DDPM) as the generative prior. RECCE [23] is a reconstruction-based deepfake forensic method, which exploits the reconstruction difference as guidance of forgery traces. Delocate [24] utilizes an MAE to learn the distribution of pristine faces for the recovery of manipulated faces. DFI [26] is a deepfake inversion method that learns the reverse mapping from the forgery face to the original face.

3) *Evaluation Metrics*: We utilize the Frechet Inception Distance (FID) and Identity Similarity (IDSIm) metrics to assess the identity recovery performance. FID is commonly

employed for evaluating image similarity, while IDSIm is specifically designed to assess the identity similarity between the reconstructed image and the original image [39]. To compute IDSIm, we leverage the pretrained FaceNet model to extract identity features from both the original and recovered target faces, followed by computing the cosine similarity between these extracted features. Additionally, we use Acc_{id} to represent the identity-based recovery accuracy. It is computed based on the identity similarity between the input face and the recovered target face. A high identity similarity implies a small discrepancy, and vice versa. If the identity similarity surpasses the threshold of 0.9, the input face is categorized as real. Otherwise, the input face is classified as fake.

4) *Implementation Details*: We employ an EfficientNet-B0 as the backbone for the ISM and a ViT16 as the backbone for the MAE network. All the face images are extracted by RetinaFace and then resized to 224×224 pixels. During training, the models are simultaneously trained on both real and forgery images. Additionally, we utilize the algorithm from BI [17] to continuously generate forgery faces and masks, which aids in enhancing the segmentation performance of the ISM. The source and target faces recovered from the real images are the real images themselves. For the forgery images, the recovered faces correspond to the source and target faces present in the dataset. We train our model using four NVIDIA 4090 GPUs. The mask ratio used in the TIRM is set as 0.5 and the patch size is set as 16. We optimize the models using the AdamW optimizer with a learning rate of $1e-4$ and a weight decay of $1e-5$. To improve the target face recovery quality, the parameters α and β are set as 2. The loss weights λ_1 , λ_2 , and λ_3 are set as 0.5.

B. Deepfake Recovery Results Analysis

We evaluate the identity recovery performance on the FaceForensics++, CelebaMegaFS and FFHQ-E4S datasets. Forgery images in the test sets are fed into DFREC to generate the recovered source and target faces. Quantitative and qualitative comparisons are made between DFREC and other face inpainting and deepfake recovery methods.

Quantitative Evaluation We use FID to assess the image recovery quality, and IDSIm to evaluate identity recovery

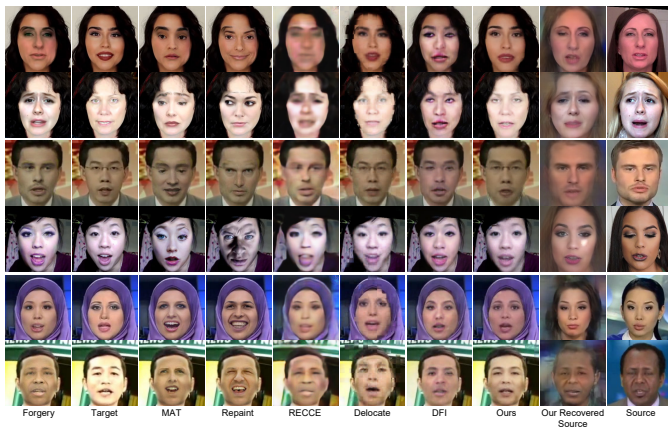


Fig. 3. Comparison of identity recovery quality of different face inpainting and deepfake recovery methods on face-swapping images of the FaceForensics++ dataset.

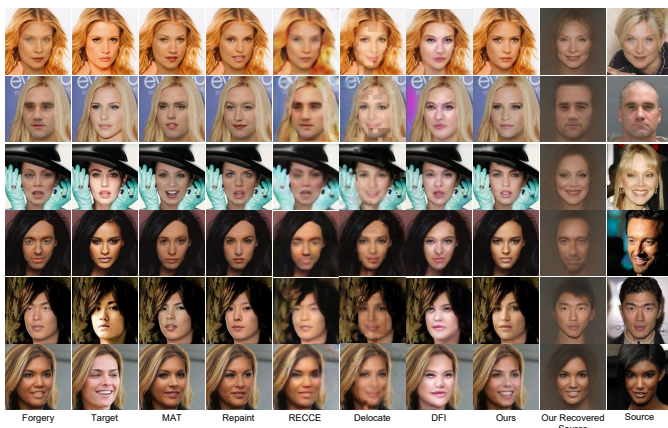


Fig. 4. Comparison of identity recovery quality of different face inpainting and deepfake recovery methods on face-swapping images of the CelebaMegaFS dataset.

quality between the recovered and the original target face for comparison with other methods. We leverage publicly available pre-trained models or existing codes for MAT, Repaint, and RECCE. Delocate and DFI are implemented by following the detailed methodologies presented in the corresponding papers. For face inpainting methods like MAT and Repaint, we employ dlib for the facial detection, and then mask areas that contain facial components before inpainting. Table I presents the recovery performance across the three datasets. The ‘None’ method in the first line shows the FID scores between the forgery face and the original target face, and the next six lines show the values of the corresponding metrics between the recovered target face and the original target face. We analyze the results of image recovery on the FaceForensics++, CelebaMegaFS, and FFHQ-E4S datasets. Compared with existing face inpainting methods [37], [38] and deepfake recovery methods [23], [24], [26], DFREC achieves the best FID scores and identity similarity in different types of face swapping forgeries, demonstrating a higher capability of generating images that are closer to the original target face identity.

Qualitative Evaluation Figures 3 - 5 compare the target

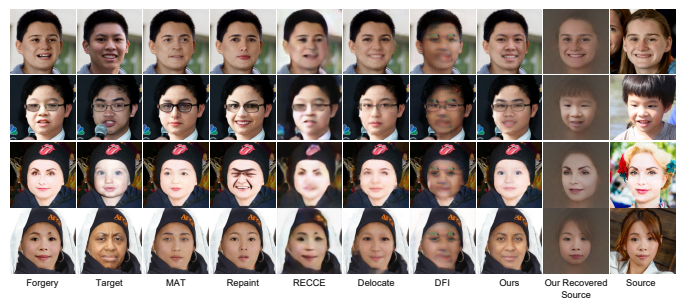


Fig. 5. Comparison of identity recovery quality of different face inpainting and deepfake recovery methods on face-swapping images of the FFHQ-E4S dataset.

TABLE II

GENERALIZATION OF DEEFAKE RECOVERY COMPARED WITH DFI [26] ACROSS DIVERSE FORGERY IMAGES. Acc_{id} IS USED AS THE EVALUATION METRIC. INTRA-DATASET EVALUATIONS ARE HIGHLIGHTED IN RED.

Method	Train	CelebaMegaFS			FaceForensics++		
		FTM	IDI	LCR	DF	FShi	LCR
DFI	C-FTM	75.20	70.43	49.03	42.32	33.01	67.96
DFREC		100.00	99.95	98.37	99.41	85.44	83.14
DFI	C-IDI	58.63	55.89	39.20	26.76	19.86	44.88
DFREC		100.00	100.00	98.73	99.78	90.30	94.38
DFI	C-LCR	91.83	89.24	94.27	75.63	64.96	77.03
DFREC		100.00	100.00	100.00	99.27	91.82	97.30

identity recovery quality between DFREC and several SOTA face inpainting and deepfake recovery methods. The evaluations were conducted on the test sets of the FaceForensics++, CelebaMegaFS, and FFHQ-E4S, respectively. As shown in Figures 3 - 5, although MAT and Repaint can synthesize realistic facial images based on the unmasked region, there are still identity gaps between the synthesized images and the original target faces. We also compared DFREC with three deepfake recovery approaches [23], [24], [26]. They tend to generate blurred and unidentified faces, which are apparently different from the original target faces. In contrast, DFREC can synthesize more realistic target faces with similar identities as the original target faces.

C. Generalization Evaluation of Deepfake Recovery

In this section, we assess the generalized deepfake recovery performance of DFREC on the FaceForensics++ and CelebaMegaFS datasets. We trained DFREC on the CelebaMegaFS dataset and then evaluate its deepfake recovery accuracy across the two datasets. Table II presents the identity-based recovery accuracy Acc_{id} on various types of forgery data. It can be observed that DFREC generally outperforms DFI [26] in terms of the generalized deepfake recovery. To visually demonstrate the generalization effect of DFREC, we present the recovered target images across different datasets in Figure 6. It can be seen that DFREC could well recover the target faces from the unseen forgery images.

D. Ablation Study

In this section, we present an ablation study conducted on the CelebaMegaFS dataset to validate the efficacy of the two

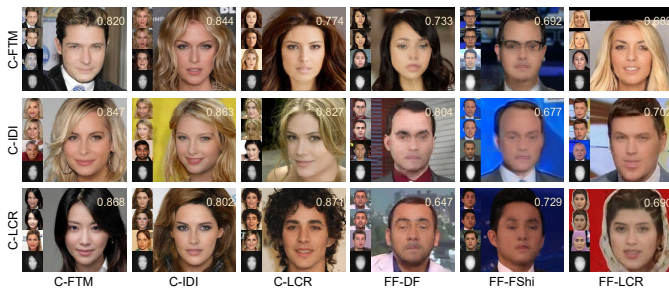


Fig. 6. Target face recovery on unseen forgeries. The vertical axis represents the training dataset, and the horizontal axis denotes the evaluation dataset. From top to bottom on the left side of the recovered images are the forged face, target face, source face, and segmentation map. The value at the top-right corner indicates the identity similarity between the recovered and target faces.

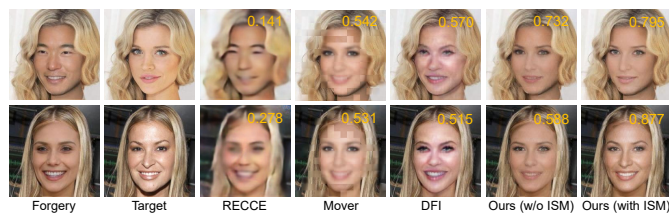


Fig. 7. Ablation experiments for the ISM. The value at the top-right corner of each recovered image indicates the identity similarity between the recovered and target faces. The images are selected from the CelebaMegaFS-LCR dataset.

key components of DFREC. We systematically dismantle the ISM and Target Identity Fusion to evaluate their individual contributions.

Identity Segmentation Module To demonstrate its significance, we remove the ISM and input the image directly to the TIRM. For the MAE of TIRM, we employ a uniform mask encompassing the entire target face region. The visualization results on the CelebaMegaFS dataset are shown in Figure 7. It shows that DFREC with ISM tends to generate more accurate target face. We also conducted quantitative evaluations on the three types of forgeries with CelebaMegaFS. The identity similarity between the recovered and the original target face is calculated and shown in Table III. The effectiveness of the ISM is corroborated by the improved identity similarity when the ISM is included.

Target Identity Fusion In DFREC, we hypothesize that the segmented source information contains target identity features. Thus, we use the SIRM to extract the target identity features and fuse them with the visible token embeddings obtained from the MAE to facilitate the target face recovery. To demonstrate its efficacy, we conduct an ablation study by removing the fusion strategy to solely rely on unmasked patches for recovery. As shown in Table III, the ability of DFREC to recover the target face is relatively weak without the fusion strategy. The improvement is significant with the fusion strategy, which attests to our hypothesis that the identity fusion plays a pivotal role in enhancing the quality of the target face recovery.

TABLE III
ABLATION EXPERIMENTS OF THE ISM AND FUSION STRATEGY. THE EVALUATIONS ARE CONDUCTED ON THE CELEBAMEGAFS IMAGES DEEPPAKED BY FTM, IDINJECTION AND LCR.

Settings		FTM		IDInjection		LCR	
ISM	Fusion	FID↓	IDSIm↑	FID↓	IDSIm↑	FID↓	IDSIm↑
		84.97	0.3241	86.94	0.3573	80.86	0.2685
✓		22.87	0.5374	23.60	0.5520	26.52	0.4591
	✓	30.53	0.5388	29.09	0.5436	32.19	0.5687
✓	✓	15.35	0.7192	13.78	0.7582	14.75	0.6967

V. CONCLUSION

This paper proposes a novel deepfake identity recovery framework, DFREC, which is capable of restoring both the source and target faces from the deepfake faces. DFREC incorporates an ISM to effectively segment the source and target face information, a SIRM to restore the source face and extract latent target identity features, and a Mask Autoencoder-based TIRM to integrate the background information with the extracted target identity features for the target face reconstruction. We conduct extensive evaluations on deepfake images generated from the FaceForensics++, CelebaMegaFS, and FFHQ-E4S datasets by six different face swapping algorithms. The results demonstrate that DFREC outperforms existing face inpainting methods and deepfake recovery approaches, confirming its potential as a forensic tool for deepfake source and target identities tracing.

REFERENCES

- [1] K. Shiohara and T. Yamasaki, “Detecting deepfakes with self-blended images,” in *Proceedings of the IEEE/CVF Conference on Computer Vision and Pattern Recognition*, 2022, pp. 18 720–18 729.
- [2] X. Dong, J. Bao, D. Chen, T. Zhang, W. Zhang, N. Yu, D. Chen, F. Wen, and B. Guo, “Protecting celebrities from deepfake with identity consistency transformer,” in *Proceedings of the IEEE/CVF Conference on Computer Vision and Pattern Recognition*, 2022, pp. 9468–9478.
- [3] B. Liu, B. Liu, M. Ding, T. Zhu, and X. Yu, “Ti2net: temporal identity inconsistency network for deepfake detection,” in *Proceedings of the IEEE/CVF Winter Conference on Applications of Computer Vision*, 2023, pp. 4691–4700.
- [4] C. Zhao, C. Wang, G. Hu, H. Chen, C. Liu, and J. Tang, “Istvt: interpretable spatial-temporal video transformer for deepfake detection,” *IEEE Transactions on Information Forensics and Security*, vol. 18, pp. 1335–1348, 2023.
- [5] L. Lin, X. He, Y. Ju, X. Wang, F. Ding, and S. Hu, “Preserving fairness generalization in deepfake detection,” in *Proceedings of the IEEE/CVF Conference on Computer Vision and Pattern Recognition*, 2024, pp. 16 815–16 825.
- [6] Z. Ba, Q. Liu, Z. Liu, S. Wu, F. Lin, L. Lu, and K. Ren, “Exposing the deception: Uncovering more forgery clues for deepfake detection,” in *Proceedings of the AAAI Conference on Artificial Intelligence*, vol. 38, no. 2, 2024, pp. 719–728.
- [7] B. Huang, Z. Wang, J. Yang, J. Ai, Q. Zou, Q. Wang, and D. Ye, “Implicit identity driven deepfake face swapping detection,” in *Proceedings of the IEEE/CVF Conference on Computer Vision and Pattern Recognition*, 2023, pp. 4490–4499.
- [8] V. Blanz, K. Scherbaum, T. Vetter, and H.-P. Seidel, “Exchanging faces in images,” in *Computer Graphics Forum*, vol. 23, no. 3. Wiley Online Library, 2004, pp. 669–676.
- [9] Y. Nirkin, I. Masi, A. T. Tuan, T. Hassner, and G. Medioni, “On face segmentation, face swapping, and face perception,” in *2018 13th IEEE International Conference on Automatic Face & Gesture Recognition (FG 2018)*. IEEE, 2018, pp. 98–105.
- [10] Y. Nirkin, Y. Keller, and T. Hassner, “Fsgan: Subject agnostic face swapping and reenactment,” in *Proceedings of the IEEE/CVF international conference on computer vision*, 2019, pp. 7184–7193.

- [11] S. Gu, J. Bao, H. Yang, D. Chen, F. Wen, and L. Yuan, "Mask-guided portrait editing with conditional gans," in *Proceedings of the IEEE/CVF conference on computer vision and pattern recognition*, 2019, pp. 3436–3445.
- [12] L. Li, J. Bao, H. Yang, D. Chen, and F. Wen, "Advancing high fidelity identity swapping for forgery detection," in *Proceedings of the IEEE/CVF conference on computer vision and pattern recognition*, 2020, pp. 5074–5083.
- [13] R. Chen, X. Chen, B. Ni, and Y. Ge, "Simsap: An efficient framework for high fidelity face swapping," in *Proceedings of the 28th ACM international conference on multimedia*, 2020, pp. 2003–2011.
- [14] Y. Zhu, Q. Li, J. Wang, C.-Z. Xu, and Z. Sun, "One shot face swapping on megapixels," in *Proceedings of the IEEE/CVF conference on computer vision and pattern recognition*, 2021, pp. 4834–4844.
- [15] C. Xu, J. Zhang, M. Hua, Q. He, Z. Yi, and Y. Liu, "Region-aware face swapping," in *Proceedings of the IEEE/CVF Conference on Computer Vision and Pattern Recognition*, 2022, pp. 7632–7641.
- [16] Z. Liu, M. Li, Y. Zhang, C. Wang, Q. Zhang, J. Wang, and Y. Nie, "Fine-grained face swapping via regional gan inversion," in *Proceedings of the IEEE/CVF conference on computer vision and pattern recognition*, 2023, pp. 8578–8587.
- [17] L. Li, J. Bao, T. Zhang, H. Yang, D. Chen, F. Wen, and B. Guo, "Face x-ray for more general face forgery detection," in *Proceedings of the IEEE/CVF conference on computer vision and pattern recognition*, 2020, pp. 5001–5010.
- [18] D. Nguyen, N. Mejri, I. P. Singh, P. Kuleshova, M. Astrid, A. Kacem, E. Ghorbel, and D. Aouada, "Laa-net: Localized artifact attention network for quality-agnostic and generalizable deepfake detection," in *Proceedings of the IEEE/CVF Conference on Computer Vision and Pattern Recognition*, 2024, pp. 17395–17405.
- [19] T. Zhao, X. Xu, M. Xu, H. Ding, Y. Xiong, and W. Xia, "Learning self-consistency for deepfake detection," in *Proceedings of the IEEE/CVF international conference on computer vision*, 2021, pp. 15023–15033.
- [20] Z. Yan, Y. Zhang, Y. Fan, and B. Wu, "Ucf: Uncovering common features for generalizable deepfake detection," in *Proceedings of the IEEE/CVF International Conference on Computer Vision*, 2023, pp. 22412–22423.
- [21] Y. Jeong, D. Kim, Y. Ro, and J. Choi, "FrepGAN: Robust deepfake detection using frequency-level perturbations," in *Proceedings of the AAAI conference on artificial intelligence*, vol. 36, no. 1, 2022, pp. 1060–1068.
- [22] Y. Wang, K. Yu, C. Chen, X. Hu, and S. Peng, "Dynamic graph learning with content-guided spatial-frequency relation reasoning for deepfake detection," in *Proceedings of the IEEE/CVF Conference on Computer Vision and Pattern Recognition*, 2023, pp. 7278–7287.
- [23] J. Cao, C. Ma, T. Yao, S. Chen, S. Ding, and X. Yang, "End-to-end reconstruction-classification learning for face forgery detection," in *Proceedings of the IEEE/CVF Conference on Computer Vision and Pattern Recognition*, 2022, pp. 4113–4122.
- [24] J. Hu, X. Liao, D. Gao, S. Tsutsui, Q. Wang, Z. Qin, and M. Z. Shou, "Delocate: Detection and localization for deepfake videos with randomly-located tampered traces," *arXiv preprint arXiv:2401.13516*, 2024.
- [25] J. Ai, Z. Wang, B. Huang, and Z. Han, "Deepreversion: Reversely inferring the original face from the deepfake face," in *2023 International Joint Conference on Neural Networks (IJCNN)*. IEEE, 2023, pp. 1–7.
- [26] J. Ai, Z. Wang, B. Huang, Z. Han, and Q. Zou, "Deepfake face provenance for proactive forensics," in *2023 IEEE International Conference on Image Processing (ICIP)*. IEEE, 2023, pp. 2025–2029.
- [27] Y. Nirkin, L. Wolf, and T. Hassner, "Hyperseg: Patch-wise hypernetwork for real-time semantic segmentation," in *Proceedings of the IEEE/CVF Conference on Computer Vision and Pattern Recognition*, 2021, pp. 4061–4070.
- [28] K. He, X. Chen, S. Xie, Y. Li, P. Dollár, and R. Girshick, "Masked autoencoders are scalable vision learners," in *Proceedings of the IEEE/CVF conference on computer vision and pattern recognition*, 2022, pp. 16000–16009.
- [29] F. Schroff, D. Kalenichenko, and J. Philbin, "Facenet: A unified embedding for face recognition and clustering," in *Proceedings of the IEEE conference on computer vision and pattern recognition*, 2015, pp. 815–823.
- [30] Q. Cao, L. Shen, W. Xie, O. M. Parkhi, and A. Zisserman, "Vggface2: A dataset for recognising faces across pose and age," in *2018 13th IEEE international conference on automatic face & gesture recognition (FG 2018)*. IEEE, 2018, pp. 67–74.
- [31] J. Deng, W. Dong, R. Socher, L.-J. Li, K. Li, and L. Fei-Fei, "Imagenet: A large-scale hierarchical image database," in *2009 IEEE Conference on Computer Vision and Pattern Recognition*. IEEE Computer Society, 2009, pp. 248–255.
- [32] K. He, Z. Wang, Y. Fu, R. Feng, Y.-G. Jiang, and X. Xue, "Adaptively weighted multi-task deep network for person attribute classification," in *Proceedings of the 25th ACM international conference on Multimedia*, 2017, pp. 1636–1644.
- [33] Z. Liu, P. Luo, X. Wang, and X. Tang, "Deep learning face attributes in the wild," in *Proceedings of International Conference on Computer Vision (ICCV)*, December 2015.
- [34] A. Rossler, D. Cozzolino, L. Verdoliva, C. Riess, J. Thies, and M. Nießner, "Faceforensics++: Learning to detect manipulated facial images," in *Proceedings of the IEEE/CVF international conference on computer vision*, 2019, pp. 1–11.
- [35] Y. Zhu, Q. Li, J. Wang, C. Xu, and Z. Sun, "One shot face swapping on megapixels," in *Proceedings of the IEEE conference on computer vision and pattern recognition (CVPR)*, June 2021, pp. 4834–4844.
- [36] T. Karras, S. Laine, and T. Aila, "A style-based generator architecture for generative adversarial networks," in *Proceedings of the IEEE/CVF conference on computer vision and pattern recognition*, 2019, pp. 4401–4410.
- [37] W. Li, Z. Lin, K. Zhou, L. Qi, Y. Wang, and J. Jia, "Mat: Mask-aware transformer for large hole image inpainting," in *Proceedings of the IEEE/CVF conference on computer vision and pattern recognition*, 2022, pp. 10758–10768.
- [38] A. Lugmayr, M. Danelljan, A. Romero, F. Yu, R. Timofte, and L. Van Gool, "Repaint: Inpainting using denoising diffusion probabilistic models," in *Proceedings of the IEEE/CVF conference on computer vision and pattern recognition*, 2022, pp. 11461–11471.
- [39] K. Shiohara, X. Yang, and T. Taketomi, "Blendface: Re-designing identity encoders for face-swapping," in *Proceedings of the IEEE/CVF International Conference on Computer Vision*, 2023, pp. 7634–7644.